MULTI-BAND SEARCH OF COALESCING BINARIES APPLIED TO VIRGO CITF DATA

F.MARION

Laboratoire de Physique des Particules (LAPP), Annecy-Le-Vieux, France

on behalf of the
VIRGO COLLABORATION
see La Penna's paper for the Virgo Collaboration authors list

An optimal search for gravitational waves emitted by compact coalescing binaries is a heavy computing task for wide-band detectors. In this article we present a method based on a multi-band template analysis that could be used to reduce the cost of such a search. A simple analysis has been performed on data recorded with the VIRGO central interferometer, both with the multi-band and standard methods. Results are reported.

1 Introduction

It is well known that searching for gravitational waves emitted by compact coalescing binaries using optimal filtering requires large computing resources. This is especially true if the search extends to low mass objects, or if the detector is sensitive enough at low frequency.

Two factors are responsible for the computing cost of such a search. One is the number of templates needed to cover the mass parameter space insuring that a large fraction of the optimal signal ratio is collected. The required number of templates is related to the duration of the longest signal, which is dominated by the slow low frequency evolution of the chirp. The second factor is the size of the fast Fourier transforms (FFT) involved in the matched filtering process. It is determined both by the signal duration and by the frequency used to sample the signal, therefore by the signal bandwidth.

It can be argued [1] that splitting the analysis in several frequency bands can reduce the computing cost. We start by recalling the principle of the multi-band template analysis (MBTA). We then present some results obtained running a test analysis on some data recorded during the last engineering run of the VIRGO central interferometer (CITF) [2]. Both the standard and multi-band searches have been applied on these data.

2 MBTA

2.1 Principle

The correlation involved in matched filtering can be most efficiently performed in the frequency domain. The basic principle of the MBTA method is to split the correlation integral in several frequency bands, as in equation 1 for two bands, with $h(f)$ the frequency representation of the signal measured by the detector, $T(f, M)$ the template used - depending on mass parameters summarized as M - and $S(t, M)$ the filtered signal obtained for this template.

$$S(t, M) = \int_{f_{min}}^{f_{max}} h(f)T(f, M)df = \int_{f_{min}}^{f_c} h(f)T(f, M)df + \int_{f_c}^{f_{max}} h(f)T(f, M)df \qquad (1)$$

Splitting the analysis in two or more frequency bands can reduce the cost associated to the template search, both because it leads to a reduction of the number of templates, and because the size of the FFTs involved in the algorithm is decreased. The reduction in the number of templates is directly related to the shortening of the signal considered in a narrower bandwidth; this is especially significant for the high frequency band. The decrease of the FFT size is due to the shorter signal again, and to the advantage that can be made of the signal limited bandwidth - in the low frequency band - by using a reduced sampling frequency. The overall expected gain depends on the search parameters (minimal mass and minimal frequency). From a simple model it has been estimated to be as high as a factor 100 for the CPU and a factor 500 for the storage, for a three bands search [1].

Equation 1 shows that the matched filtering procedure is applied on each of the frequency bands, with the consequence that the corresponding results can be used to analyze each band independently. This makes the method especially suited to a hierarchical search, with the first step of the search based on the reduced bands. It also allows to apply consistency checks on candidates stemming from the algorithm, such as a χ^2 test [3] of the signal consistency with a chirp in the frequency domain.

Equation 1 is written in a way which implies that a coherent combination of the filtered signals obtained with the reduced bands can be performed to obtain the same signal as would come out of a full band filtering. It is indeed the case, but needs to be discussed in more details, since the maximization over arrival time and phase performed on the filtered signal make things slightly more complex.

2.2 Coherent combination

As usual, while the maximization over arrival time of the filtered signal is performed in a straightforward way, the maximization over the initial phase is handled by using a couple of templates in quadrature for each point in the mass parameter space and computing a quadratic sum of the signals obtained with both templates (equation 2).

$$S(t) = \sqrt{S_{0°}(t)^2 + S_{90°}(t)^2} \qquad (2)$$

To be coherent, the combination of the different bands has to be done at the level of each template before the quadratic sum is taken. As a consequence of the phase evolution of the chirp, the signal enters the different frequency bands at different times and with different initial phases. Therefore the signals have to be shifted both in time (translation) and in phase (rotation) before being summed, as in equation 3 (for two bands).

$$S_{0°}(t) = S_{0°LF}(t) + \cos(\Delta\phi)S_{0°HF}(t + \Delta t) + \sin(\Delta\phi)S_{90°HF}(t + \Delta t) \qquad (3)$$

The combination parameters - time and phase shifts Δt and $\Delta\phi$ - depend on the template mass parameters and are computed a priori.

2.3 Algorithm development

Following a preliminary study which demonstrated the feasibility and advantages of the multi-band method, a prototype implementation for the algorithm has been developed. It is based on several distinct template banks associated to each frequency band (templates actually used to perform the matched filtering) and to the full band (templates used only for the combination).

The processing of the data is such that the matched filters for the reduced bands are applied in parallel to the data, and the combination is done next, either systematically in the case of a flat search, or triggered by the results of a search performed on the reduced bands in the case of a hierarchical search.

A first version of the implemented algorithm being now available, it has to undergo several tests. One important point is to measure the gain that can actually be obtained from a multi-band analysis in realistic conditions. This requires an effective and reliable algorithm to generate template grids in the mass parameter space. Such an algorithm is currently under development [4]. The behavior of the algorithm has also to be tested both on simulated and on real data. In the next section we report on a simple test analysis that was led on data collected with the VIRGO CITF.

3 Test analysis with VIRGO CITF data

Some data recorded during the last engineering run held during the commissioning of the VIRGO CITF have been used as a test bench for a simple analysis using the MBTA algorithm. The goal was both to get a flavor of the detector noise performance and to check the robustness of the algorithm in a real data environment.

3.1 Data sample

The period analyzed has been selected in order to get a data sample for which fairly good quality can be expected. It consists of a long segment (almost 10 hours) for which both the interferometer and the output mode cleaner were continuously locked. The data were recorded during night operation. Of this data segment, only five short periods (about 1 minute each) have been vetoed a priori, corresponding to realignment occurrences.

3.2 Analysis configuration

Since the goal was to lead a simple exploratory analysis, the latter has been done in a very simple configuration and in particular was based on a single template. Most results are shown for a $(3\ M_\odot, 3\ M_\odot)$ template, generated using a Taylor expansion at order PN2 [5]. The analysis was done both with a single band search, based on the [50 Hz, 2 kHz] bandwidth, and with a two bands search, using the same bandwidth split at 500 Hz to share the signal to noise ratio (SNR) between the two bands.

In both cases, the analysis is run on raw data, calibrated in the frequency domain, using time dependent calibration constants. The noise level is monitored to follow up non stationarities, and events with SNR exceeding a given threshold are recorded for statistical analysis.

For the two bands search, a χ^2 variable is also computed testing the consistency of the SNR contributions from both frequency bands with that expected for a true chirp.

3.3 Horizon distance

We first assess the sensitivity of the detector to such coalescing binaries events, by measuring the maximum distance for the location of optimally oriented sources to be detected with a SNR

of at least 8. The evolution of this horizon distance as a function of time is shown on figure 1 for sources of $(1.4\ M_\odot, 1.4\ M_\odot)$, $(3\ M_\odot, 3\ M_\odot)$ and $(10\ M_\odot, 10\ M_\odot)$.
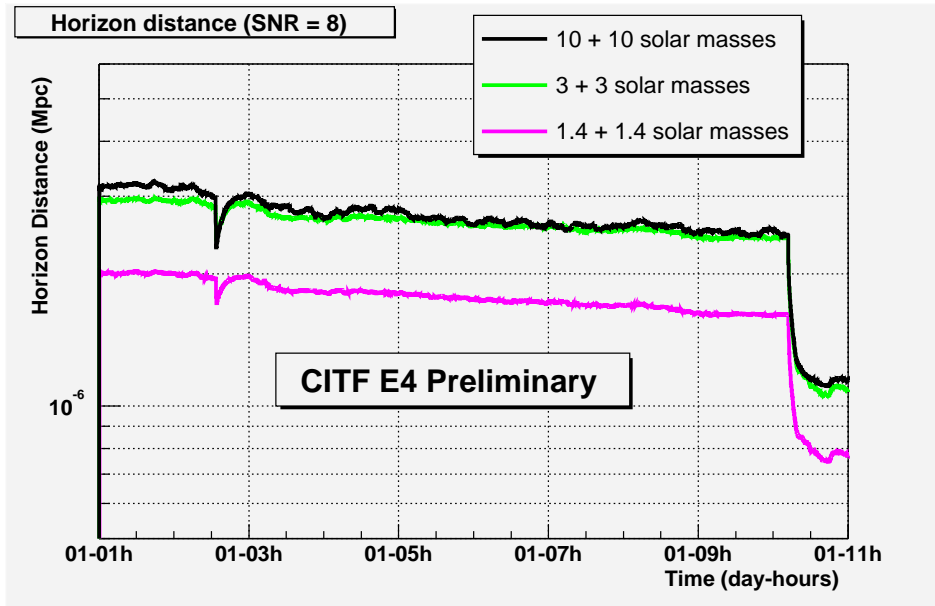

Figure 1: Farthest distance of optimally oriented sources of various masses to yield a SNR of at least 8, measured as a function of time during part of the VIRGO CITF engineering run E4.

The horizon distance increases with the source mass when comparing the $3\ M_\odot$ case to the $1.4\ M_\odot$ case, as expected. On the other hand, the horizon distance does not significantly increase when going from $3\ M_\odot$ to $10\ M_\odot$, because of the reduced bandwidth of a $10\ M_\odot$ signal, due to the relatively low value of the last stable orbit frequency.

Figure 1 shows a slow decrease of the horizon distance with time, corresponding to a gradual increase of the detector noise level. Moreover, two periods with a sharp drop in the horizon distance are clearly visible. They evidence sudden worsenings of the detector sensitivity following human actions on the injection system. Vetoes are applied on these two periods in the following search for candidates.

3.4 Observed candidates

Events with a SNR exceeding a threshold of 5 have been recorded. Figure 2 shows the distribution of the SNR as well as the evolution as a function of time of the trigger rate, namely the number of candidates recorded per second, both for the single band and for the two bands analyzes.

The obtained SNR distribution is rather restrained, with no tail extending to very large values, the strongest candidate showing a SNR of 9. Moreover, the evolution of the trigger rate is fairly uniform, with no large burst of events. These plots show that once the very simple vetoes mentioned above have been applied, the detector shows quite a regular behavior on the selected data sample.

A comparison of the distributions obtained for the single band and the two bands analyzes shows that they are consistent. A more detailed comparison of the two analyzes is given in figure 3 which shows a comparison of the SNR obtained in each case for the events present in both sets, associated on the criterion of their occurrence time. The association rate is around 80%. The missed associations are due to the dispersion of the SNR which leads to some events being above threshold in one case and below in the other case. Notwithstanding this dispersion
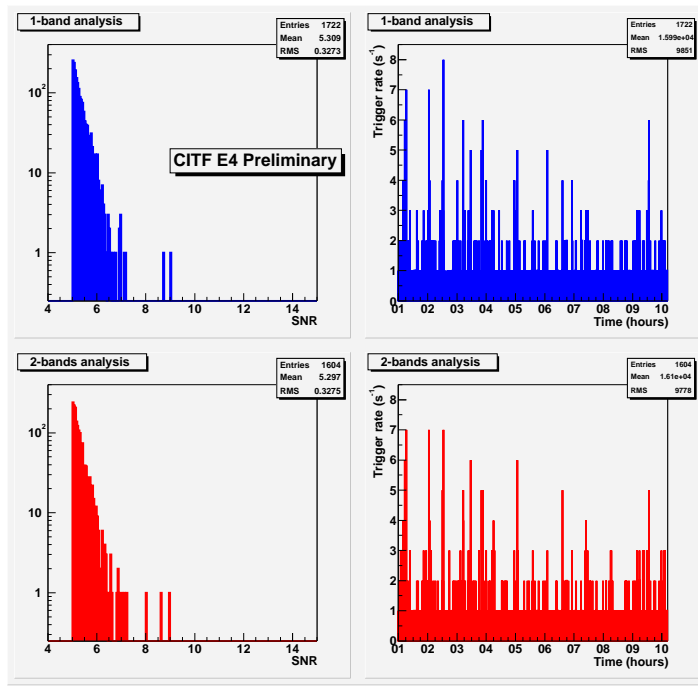
Figure 2: SNR distribution (left) and trigger rate evolution (right) for selected candidates, both for the single band analysis (top) and for the two bands analysis (bottom).

(expected from the different data slicing involved in both analyzes) the correlation of the SNR in both cases is fairly good.
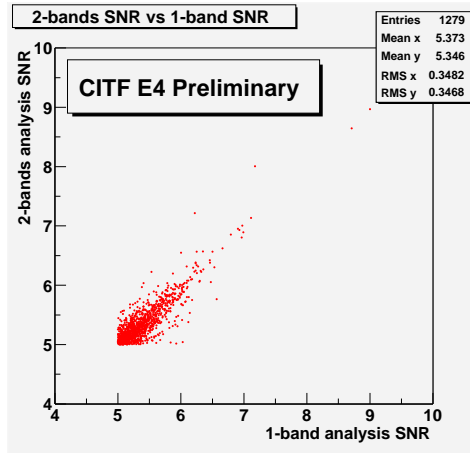

Figure 3: Comparison of the SNR measured by the single band analysis and the two bands analysis, for candidates selected by both analyzes.

We finally address the issue of vetoing some of the candidates using the χ^2 test available in the two bands analysis. Figure 4 shows how the χ^2 is distributed versus the event SNR, as well as the SNR distribution after a cut $\chi^2 < 10$ has been applied. The effect of this cut is not dramatic since we start from a SNR distribution which is already free of large tails. Nevertheless, the χ^2 cut is able to dismiss the two strongest candidates, which are two degeneracies of a single noisy event occurring at that time. This event, when observed in the time-frequency domain, corresponds to a sudden increase of the detector noise level in a narrow frequency bandwidth located around 1100 Hz. Such a narrow bandwidth is inconsistent with the signal expected from
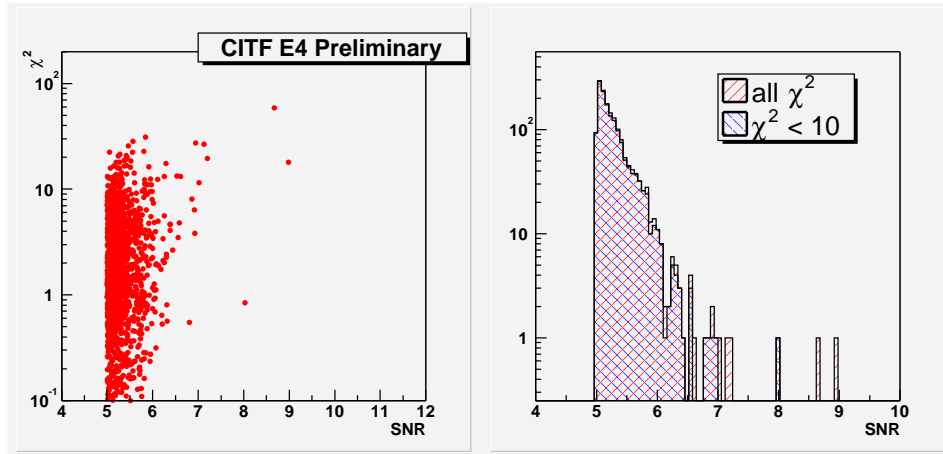
a true chirp, as evidenced by the bad χ^2.

Figure 4: Left: χ^2 distribution versus SNR for the candidates selected by the two bands analyzes. Right: Evolution of the SNR distribution after a cut on the χ^2 is applied.

On the other hand, the next strongest event (with SNR 8) corresponds to a small χ^2 value reflecting the fact it is due to a noise excess more spread on the bandwidth. It cannot therefore be dismissed by this simple test, which does not rule out the possibility that a more detailed test, based on a χ^2 with more degrees of freedom - more frequency bands - could succeed in vetoing it. Moreover, no attempt has been made here to use the detector auxiliary channels to try and reveal any associated disturbance that could be used as a veto.

4   Conclusion

An algorithm to perform a template based search for coalescing binaries is being developed. This algorithm supports multi-band analyzes expected to reduce the search cost. It has been tested on data collected with the VIRGO central interferometer, showing a fairly regular noise behavior of the detector on a selected data sample. Further work will concentrate on dealing better with the data quality and non-stationarities. The gain actually brought by a multi-band search mode will also be measured in realistic conditions.

References

1. F. Marion and B. Mours, *Gravitational Wave Data Analysis Workshop 2001*, Trento, Italy, *http://gwdaw2001.science.unitn.it/*.
2. VIRGO Collaboration, *Commissioning the central interferometer of the gravitational wave detector Virgo*, in preparation
3. B. Allen *et al*, *Phys. Rev. Lett.* **83**, 1498 (1999).
4. F. Beauville *et al*, *Gravitational Wave Data Analysis Workshop 2002*, Kyoto, Japan, *proceedings submitted to Class. Quan. Grav.*
5. D. Buskulic, G. Cella, T. Cokelaer, G.M. Guidi and A. Viceré, *The inspiral library User's manual*, VIR-MAN-CAS-7500-16, v0r4